Shallow cumulus convection: a validation of large-eddy simulation against aircraft and Landsat observations.

R. A. J. NEGGERS*
Royal Netherlands Meteorological Institute (KNMI), De Bilt, the Netherlands

P. G. DUYNKERKE† AND S. M. A. RODTS
Institute for Marine and Atmospheric Research Utrecht (IMAU), University of Utrecht, the Netherlands

1. Introduction

In the last decades, large-eddy simulation (LES) has become an important new tool in boundary layer research. It has already been used widely to study the turbulent structure of clear and cloudy boundary layers. Although encouraging, some important LES results on cumulus clouds still remain unsupported by observations, mainly due to the scarcity of suitable in-cloud measurements. For example, evaluating the 'top-hat' cloud-average thermodynamics and turbulence of LES against observations requires measurements in many natural clouds of all sizes at various heights in a small window of time. Another important issue in the parameterization of cumulus convection is the mixing between shallow cumulus clouds and the dry air of their surrounding environment.

In this study LES results on shallow cumulus convection are directly evaluated against in-cloud measurements by the NCAR C-130 aircraft during the Small Cumulus Microphysics Study (SCMS) in Florida, August 1995. An LES case is constructed based on data from surface-instruments and radiosondes of a certain day during this campaign, on which a diurnal cycle over land was observed. Of both the LES and the aircraft data, conditionally sampled averages of first and second order moments of thermodynamic and turbulent properties are calculated. Furthermore the lateral entrainment rates and the simplified budget equation for the vertical velocity are evaluated. Finally, cloud size distributions are derived from LES and compared to similar distributions obtained from a corresponding high-resolution Landsat 5 image of the SCMS area.

*Corresponding author address: Royal Netherlands Meteorological Institute (KNMI), P.O.Box 201, 3730 AE De Bilt, the Netherlands. e-mail: neggers@knmi.nl

†Deceased January 18, 2002

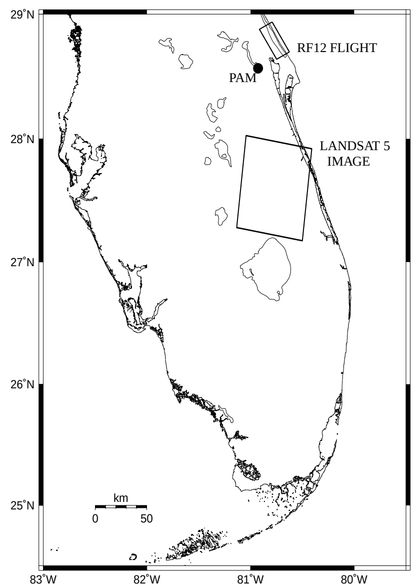

FIGURE 1: A map of Florida. The SCMS campaign was situated near Cocoa Beach, Cape Canaveral. The ground-stations PAM1 and PAM3 are indicated by the black dots. The area of flight RF12 and the area covered by the Landsat 5 image are indicated by the rectangles.

2. SCMS

The Small Cumulus Microphysics Study (SCMS) took place from July 17 until August 13, 1995 in Florida, near Cocoa Beach just north of Cape Canaveral (see Fig.1). On August 5 a clear convective boundary layer over land developed in the early morning. It deepened in time, and during the course of the morning a shallow cumulus cloud layer developed. The clouds were categorized as shallow non-precipitating cumulus with a cloud fraction of 10-20 %. This particular 'golden day' was part of a period in which persistently every day a shallow cumulus topped boundary layer developed. Observations of the geometrical and microphysical structure of the cumulus clouds in this period in SCMS have been reported

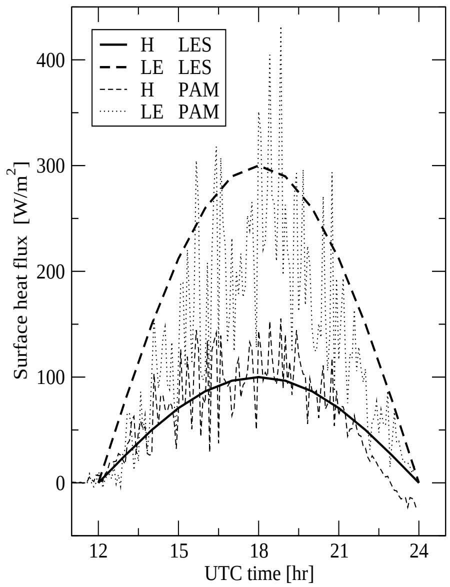

FIGURE 2: The surface latent and sensible heat fluxes as measured by the PAM station. The idealized surface fluxes imposed on LES are also plotted.

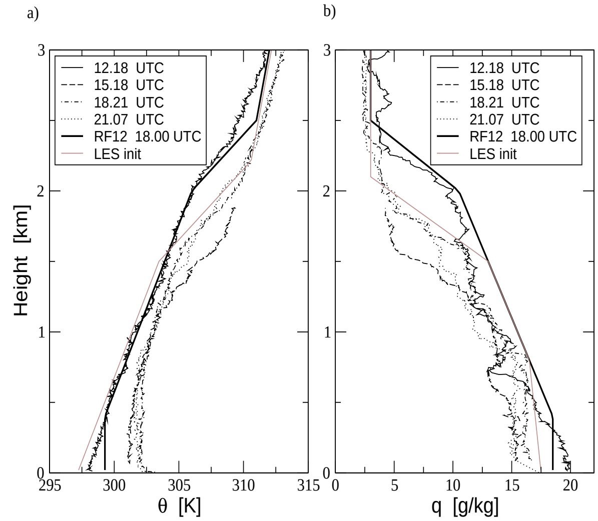

FIGURE 3: Radiosonde soundings of a) the potential temperature θ and b) the specific humidity q near station PAM3. The idealized profiles based on the vertical ascent of flight RF12 at 18:00 UTC are plotted as black solid lines, and the initial LES profiles at 12:00 UTC as grey solid lines.

by Knight and Miller (1998) and French et al. (1999). The large scale conditions did not change significantly during this period, nor where they very large compared to the local forcing by the surface fluxes. These conditions make August 5 a suitable day on which to base an LES case.

A portable meteorological station of the flux-PAM type were employed in the SCMS campaign, for a detailed description see Horst and Oncley (1995) and Militzer et al. (1995). It was situated about 50 km inland to the west of Cape Canaveral (see Fig.1). It measured the near-surface fluxes of momentum, virtual temperature and water vapor. The corresponding timeseries are plotted in Fig.2. The temperature and humidity were measured at a height of 2m. Near the PAM station radiosondes were released at intervals of approximately 3 hours, giving the vertical profiles of the temperature, specific humidity, wind-direction and wind-speed (see Fig.3).

The C-130 operated by the National Center for Atmospheric Research (NCAR) carried instruments measuring turbulence, thermodynamics and microphysics. A detailed description of the instrumentation on this aircraft and the statistical quality of the resulting cloud-averages is given by Rodts et al. (2002). The liquid water content (q_l) of the clouds is obtained from a Particle Volume Monitor (PVM) (Gerber et al. 2001). Immediately after take-off, the aircraft made a vertical sounding up to 4 km, giving the vertical profiles of the temperature and specific humidity in the flight area. This was followed by a descent to lower altitudes where the clouds were located. Three consecutive hours of measurements through the whole cloud layer then followed. The area of flight RF12 on August 5 is shown in Fig.1. These measurements are used to calculate the conditionally averaged cloud-profiles in the cloud layer.

3. The LES case

The aim is to construct a case for LES of which the development in time stays as close as possible to the range of different kind of measurements made during the day. Once that is achieved, the resulting cloud properties can be studied and compared to the available in-cloud observations in detail. Unfortunately no detailed measurements were available of the radiative and large scale forcings on the boundary layer in SCMS. Therefore, the LES case is designed to reproduce the heights of cloud base, cloud top and the inversion as observed by the aircraft and the radiosondes, using the large scale tendencies as a tool for calibration and the radiosonde profiles and the measured surface time-series as a constraint. The resulting initial profiles are displayed in Fig.3. A sinusoid shape is assumed for the surface sensible and latent heat fluxes, see Fig.2. After several test runs a net temperature forcing of -3 K/day is assumed. The moisture forcing is set to zero. A more detailed description of the LES case is given by Neggers et al. (2002b)

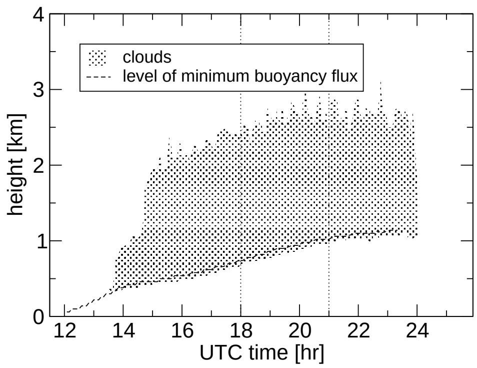

FIGURE 4: The development of the cloud layer in time in LES. The level of minimum buoyancy flux is plotted to indicate the top of the well-mixed dry-convective layer.

4. Results

The LES model used in this study is described in detail in Cuijpers and Duynkerke (1993). The LES simulation was performed on a domain of 6.4km x 6.4km x 5km. The corresponding grid-spacing was 50m x 50m x 40m. A period of 12 hours was simulated, covering the day-time cycle from 07:00 to 19:00 local time (which corresponds to 12:00 UTC to 00:00 UTC). In order to get reliable statistics, all cloud averages are calculated over the three-hour period from 18:00 to 21:00 UTC during which the in-cloud measurements were taken by flight RF12. The resulting cloud layer in LES is shown in Fig.4.

Figures 5 and 6 show that given the correct initial and boundary conditions LES reproduces the observed cloud-average thermodynamic variables of temperature, moisture and liquid water content, as well as the marginal positive cloud-average buoyancy. Furthermore the vertical component of the in-cloud turbulent kinetic energy (TKE) in LES agrees remarkably well with the observations in SCMS, see Fig.7a. Finally, cloud size distributions were derived from the vertically projected cloud populations of both LES and the Landsat image. First the size of each cloud was calculated as the square-root of its vertically projected area, after which the histograms could be built (Neggers et al. 2002). Figure 7b illustrates that the powerlaw-exponents at the smaller sizes in LES and Landsat are comparable. In both LES and Landsat this scaling regime is bounded by a scale-break, at approximately the same cloud size.

Two well-known parameterizations for shallow cumulus which make use of conditionally sampled fields were tested on the SCMS data. The lateral mixing rate of the

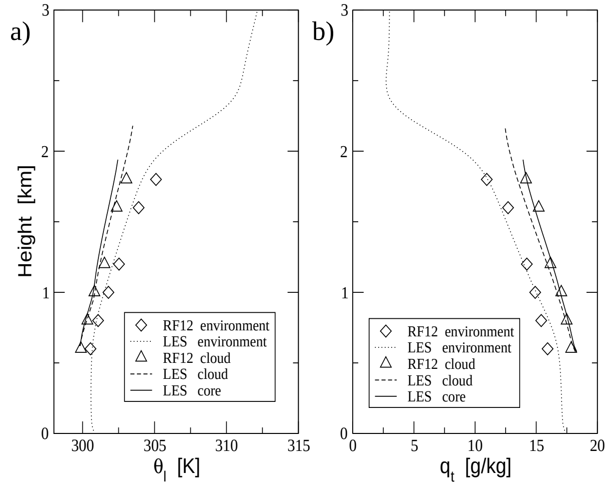

FIGURE 5: a) The liquid water potential temperature θ_l and b) the total specific humidity q_t. The cloud core is defined as the fraction of the cloudy area which is also positively buoyant.

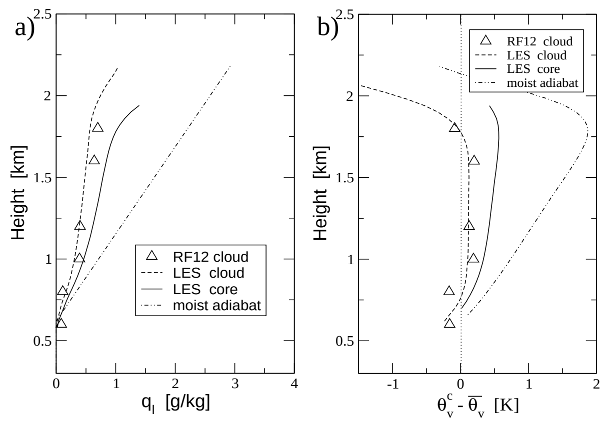

FIGURE 6: a) The liquid water content q_l^c and b) the virtual potential temperature excess of the clouds over the environment $\theta_v^c - \overline{\theta_v}$. The moist adiabat starts at cloud base.

cloud ensemble ϵ is defined by

$$\frac{\partial \phi^c}{\partial z} \;=\; -\epsilon \, \left(\phi^c - \overline{\phi}\,\right) \qquad (1)$$

The superscript c denotes the average over all the clouds at a certain height. ϕ can be one of the variables θ_l or q_t conserved for moist adiabatic ascent. Siebesma and Cuijpers (1995) first used (1) to calculate lateral entrainment rates in LES. Figure 8a shows that the magnitude and the decrease with height of ϵ calculated from the SCMS data confirm the LES results. The use of q_t in (1) gives a somewhat smaller entrainment rate.

Simpson and Wiggert (1969) formulated a simplified budget equation for the cloud vertical velocity,

$$\frac{1}{2}\frac{\partial}{\partial z}(w^c)^2 \;=\; -\beta\epsilon^c(w^c)^2 \;+\; \alpha B^c, \qquad (2)$$

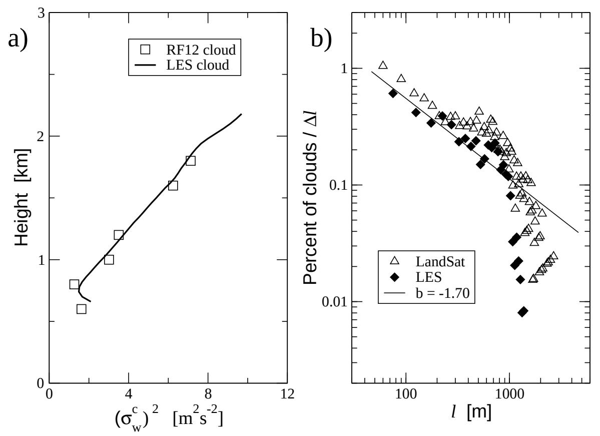

FIGURE 7: a) The cloud-average vertical velocity variance σ_w^2. b) Log-log scale plot of the cloud size density $\mathcal{N}(l)$. The solid line represents the fit $\mathcal{N}(l) \sim l^{-1.70}$.

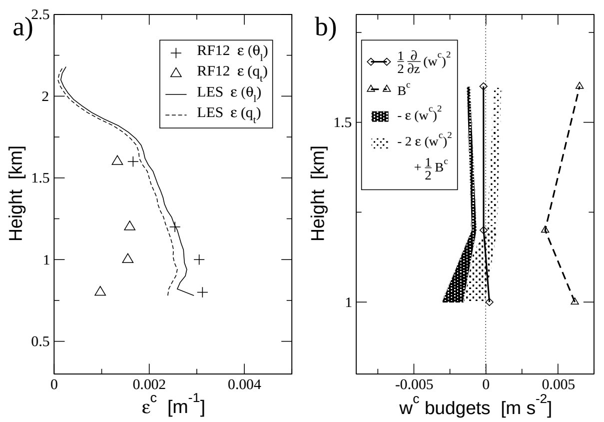

FIGURE 8: a) Lateral entrainment rates based ϵ of $\{\theta_l, q_t\}$. b) The simplified budget equation (2) for the vertical velocity of the cloud, based on RF12 data. The shaded areas represent the range between the entrainment rates resulting from the use of $\{\theta_l, q_t\}$ in (1).

This equation states that the average vertical acceleration of the cloud is controlled by buoyancy B^c minus lateral mixing. The mixing term is enhanced by a factor β to account for the impact of pressure perturbations. The buoyancy is reduced by a factor α to account for loss of potential (gravitational) energy to sub-plume turbulence. Simpson and Wiggert (1969) suggested $\beta = 2$ and $\alpha = \frac{2}{3}$. The operational ECMWF model uses $\alpha = \frac{1}{3}$, and as an intermediate we choose $\alpha = \frac{1}{2}$. Figure 8b illustrates that for the SCMS measurements the budget (2) is reasonably closed, reproducing the observed small cloud-average vertical acceleration at the heights were the cloud is positively buoyant.

5. Conclusions

These results support the credibility of the resolved thermodynamics and turbulence in LES in general, and encourage its use as a tool for testing hypotheses and developing parameterizations of shallow cumulus cloud processes. For example, the typical lateral entrainment rates found in LES are supported by the in-cloud measurements in SCMS. Secondly, the simplified budget equation of Simpson and Wiggert (1969) proved to be reasonably closed for these data.

The evaluation of the cloud size density showed that next to realistic cloud ensemble averages LES produces realistic shallow cumulus populations. The comparison between Landsat and LES emphasizes the universality of the functional form which describes the cloud size density in shallow cumulus cloud populations (see Neggers et al. 2002)

Acknowledgments The SCMS data were kindly provided by Dr. C. A. Knight. We acknowledge NCAR and its sponsor, the National Science Foundation, for the use of the observational data. The LES results in this study were obtained using the supercomputer facilities of the European Centre for Medium-Range Weather Forecasts (ECMWF) in Reading, UK. This study has been supported by the Netherlands Organization for Scientific Research under Grant 750.198.06.

REFERENCES

Cuijpers, J. W. M., and P. G. Duynkerke, 1993: Large-eddy simulation of trade-wind cumulus clouds. *J. Atmos. Sci.*, **50**, 3894-3908.

French, J. R., G. Vali and R. D. Kelly, 1999: Evolution of small cumulus clouds in Florida: observations of pulsating growth. *Atmospheric Research*, **52**, 143-165.

Gerber, H., J. B. Jensen, A. B. Davis, A. Marshak, and W. J. Wiscombe, 2001: Spectral density of cloud liquid water content at high frequencies. *J. Atmos. Sci.*, **58**, 497-503.

Horst, T.W., and S.P. Oncley, 1995: Flux-PAM measurement of scalar fluxes using cospectral similarity. Proceedings of the 9th Symposium on Meteorological Measurements and Instrumentation, March 27–31, Charlotte, NC, 495–500.

Knight, C. A. and L. J. Miller, 1998: Early radar echoes from small, warm cumulus: Bragg and hydrometeor scattering. *J. Atmos. Sci.*, **55**, 2974-2992.

Militzer, J.M., M.C. Michaelis, S.R. Semmer, K.S. Norris, T.W. Horst, S.P. Oncley, A.C. Delany, and F.V. Brock, 1995: Development of the prototype PAM III/Flux-PAM surface meteorological station. Proceedings of the 9th Symposium on Meteorological Measurements and Instrumentation, March 27–31, Charlotte, NC, pp 490–494.

Neggers, R. A. J., A. P. Siebesma and H. J. J. Jonker, 2002: Statistics of cumulus cloud populations in large-eddy simulations. *Accepted by the J. Atmos. Sci.*

Neggers, R. A. J., P. G. Duynkerke and S. M. A. Rodts, 2002b: Shallow cumulus convection: a validation of large-eddy simulation against aircraft and Landsat observations. *Submitted to the Q. J. Roy. Met. Soc.*

Rodts, S. M. A., P. G. Duynkerke, and H. J. J. Jonker, 2002: Size distributions and dynamical properties of shallow cumulus clouds from aircraft measurements and satellite data. *Submitted to J. Atmos. Sci.*

Siebesma, A. P., and J. W. M. Cuijpers, 1995: Evaluation of parametric assumptions for shallow cumulus convection. *J. Atmos. Sci.*, **52**, 650-666.

Siebesma, A. P., et al., 2002: An intercomparison study for cloud resolving models of shallow cumulus convection. *Submitted to J. Atmos. Sci.*

Simpson, J., and V. Wiggert, 1969: Models of precipitating cumulus towers. *Mon. Wea. Rev.*, **97**, 471-489.